Thermochimica Acta, 197 (1992) 443–451
Elsevier Science Publishers B.V., Amsterdam

Synthetic reversible oxygen- or nitrogen-carrying chelates of nickel(II)

A. Busnot, J.F. Le Querler and J. Yazbeck

Laboratoire de Chimie Minérale et Bioinorganique, U.F.R. de Sciences, Université de Caen, Esplanade de la Paix, 14032 Caen Cedex (France)

(Received 7 July 1991)

Abstract

New oxygenated complexes of nickel(II) with the composition $Ni_2O_4(Imid)_xA_y \cdot zNH_3$ or $Ni_2N_4(Imid)_{x'}A_{y'} \cdot z'NH_3$, where Imid represents the imidazole molecule and A the anion of succinic acid, maleic acid or glutaric acid, have been synthesized. The behavior of these salts when heated in air has been studied by thermogravimetric methods and it has been established that in all cases the product of the decomposition is the oxide or the carbonate.

Diffuse reflectance spectra are presented. Calculated electronic transitions are in good agreement with those observed. It seems that the nickel ions are in an octahedral environment.

INTRODUCTION

Coordination compounds of transition metals with molecular oxygen are currently being studied [1–8]. In a number of cases, these coordination compounds can activate molecular oxygen and catalyse oxidations. Synthetic reversible oxygen-carrying chelates, i.e., chelates that can take up and release molecular oxygen reversibly, have been of interest as model compounds in the study of the reversible mechanisms involved in the very complex natural oxygen carriers, e.g. the hemoglobins and hemocyanins, and as a means of separating molecular oxygen from the air. Much of the recent activity in this area has been motivated by a desire to elucidate the factors which lead to reversible O_2 binding, and to understand the transport of O_2 and oxidations by it in biological systems. Systematic approaches to these problems will require an understanding of the electronic nature of the coordinated O_2 fragment.

Reversible oxygen sorption has been observed in a number of aminoacid and dipeptide complexes of Co(II) [9]. Recently, several oxygen-carrying

---

Correspondence to: A. Busnot, Laboratoire de Chimie Minérale et Bioinorganique, U.F.R. de Sciences, Université de Caen, Esplanade de la Paix, 14032 Caen Cedex, France.

TABLE 1

Microanalysis results

Compound	Element	Theoretical, %	Experimental, %
A	C	32.7	33.5
	H	6.2	5.3
	N	25.1	25.0
	Ni	8.4	8.8
B	C	33.36	33.7
	H	5.9	4.9
	N	24.96	25.3
	Ni	8.37	8.7
C	C	32.91	33.3
	H	5.6	5.3
	N	25.26	25.4
	Ni	8.47	9.3
D	C	33.66	33.7
	H	4.8	5.5
	N	25.1	25.6
	Ni	8.44	9.1
E	C	32.99	33.0
	H	6.7	5.4
	N	24.7	25.6
	Ni	8.3	8.8

chelates containing coordinating ions other than cobalt have been reported [10], but only a limited number of publications are related to the nickel complexes. Accordingly, we have directed our initial efforts toward a study of these complexes or analogous complexes containing nitrogen labile molecules.

EXPERIMENTAL AND RESULTS

Preparation

Five complexes have been prepared, involving Ni(II) succinate, Ni(II) maleate or Ni(II) glutarate and imidazole (Imid).

The following compounds were obtained (Table 1): (A) $Ni_2O_4(Imid)_6(succinate)_5 \cdot 13NH_3$, (B) $Ni_2N_4(Imid)_5(succinate)_6 \cdot 11NH_3$, (C) $Ni_2O_4(Imid)_6(maleate)_5 \cdot 13NH_3$, (D) $Ni_2N_4(Imid)_5(maleate)_6 \cdot 11NH_3$, and (E) $Ni_2N_4(Imid)_3(glutarate)_6 \cdot 15NH_3$. A mixture of imidazole (2.5×10^{-2} mol) and nickel(II) sulfate (10^{-2} mol) in ammoniacal medium (6M) was subjected to magnetic stirring and then filtered. The solution was kept under an O_2 or a N_2 flow for 5 minutes and then filtered. The solution so obtained was treated with a dicarboxylic acid (2.5×10^{-2} mol) and then left for crystallization at 278 K.

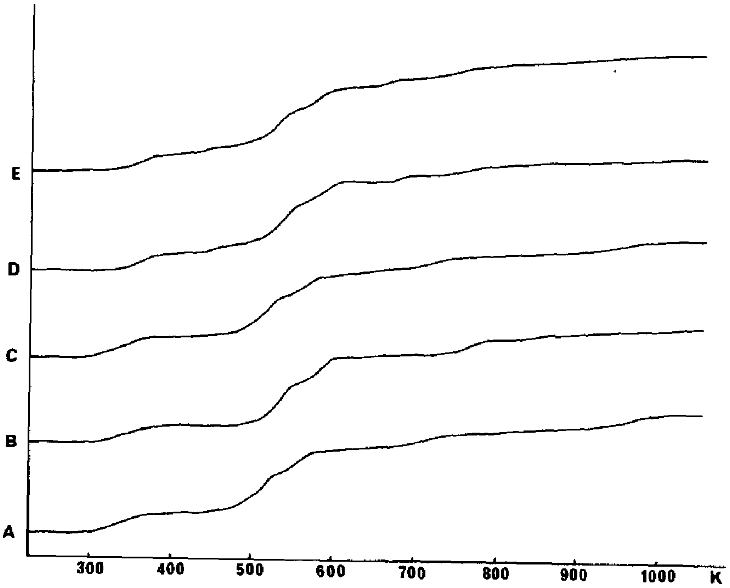

Fig. 1. TG curves in air.

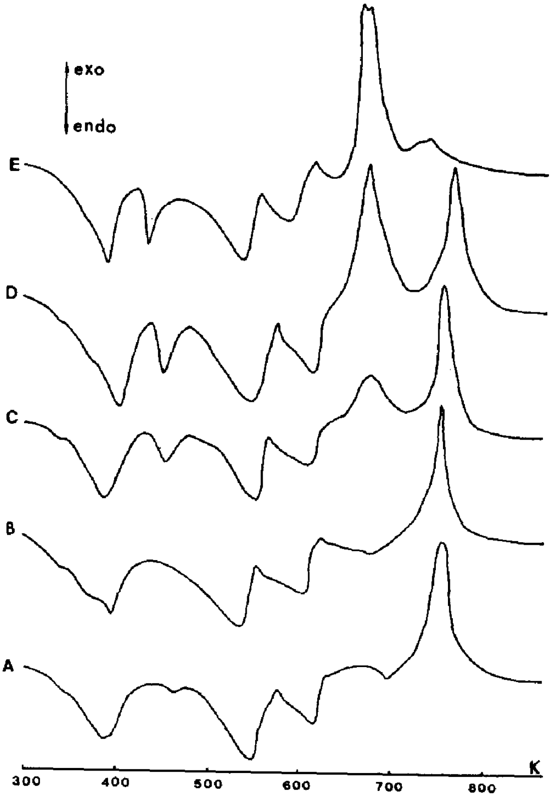

Fig. 2. Differential thermal curves in air.

EXHIBIT 1
Decomposition of the complexes

Compound A

$$\xrightarrow[\text{DTA(endo) 358 K}]{\text{TG 307–371 K}} \mathrm{Ni_2O_4(Imid)_6(succinate)_5 \cdot 2NH_3}$$

WL %th. 13.4
WL %exp. 12.6

$$\xrightarrow[\text{DTA(endo) 391 K}]{\text{TG 371–435 K}} \mathrm{Ni_2O_4(Imid)_6(succinate)_5}$$

WL %th. 2.45
WL %exp. 2.4

$$\xrightarrow[\text{DTA(endo) 463 K}]{\text{TG 435–522 K}} \mathrm{Ni_2O_2(Imid)_4(succinate)_3}$$

WL %th. 28.8
WL exp. 28.5

$$\xrightarrow[\text{DTA(endo) 545 K}]{\text{TG 522–581 K}} \mathrm{2[NiO, Imid, succinate]}$$

WL %th. 18.13
WL %exp. 17.7

$$\xrightarrow[\text{DTA(endo) 616 K}]{\text{TG 581–725 K}} \mathrm{2[Ni(CH_2{-}COO)_2]}$$

WL %th. 12.04
WL %exp. 13.1

$$\xrightarrow[\text{DTA(exo) 763 K}]{\text{TG 725–831 K}} \mathrm{NiCO_3 + NiO}$$

WL %th. 11.2
WL %exp. 13.2

Total weight loss: theoretical 86.02%; experimental 87.5%

Compound B

$$\xrightarrow[\text{DTA(endo) 400 K}]{\text{TG 307–417 K}} \mathrm{Ni_2N_4(Imid)_5(succinate)_6}$$

WL %th. 13.3
WL %exp. 12.4

$$\xrightarrow[\text{DTA(endo) 553 K}]{\text{TG 417–555 K}} \mathrm{Ni_2(Imid)_5(succinate)_3}$$

WL %th. 29.23
WL %exp. 29.3

$$\xrightarrow[\text{DTA(endo) 628 K}]{\text{TG 555–600 K}} \mathrm{Ni_2(Imid)(succinate)_3}$$

WL %th. 19.4
WL %exp. 19.7

$$\xrightarrow[\text{DTA(endo) 703 K}]{\text{TG 600–774 K}} \mathrm{2[Ni(CH_2{-}COO)_2]}$$

WL %th. 13.12
WL %exp. 13.3

$$\xrightarrow[\text{DTA(exo) 773 K}]{\text{TG 774–831 K}} \mathrm{NiCO_3 + Ni(CH_2{-}COO)_2}$$

WL %th. 3.99
WL %exp. 4.1

$$\xrightarrow{\text{TG 831 K}} \mathrm{2NiCO_3}$$

WL %th. 3.99
WL %exp. 4.4

Total weight loss: theoretical 82.9%; experimental 83.6%.

Compound (C)

$\xrightarrow[\text{DTA(endo) 343 K}]{\text{TG 307–386 K}} \mathrm{Ni_2O_4(Imid)_6(maleate)_5NH_3} \xrightarrow[\text{DTA(endo)388–450 K}]{\text{TG 386–531 K}} \mathrm{Ni_2O_4(Imid)_4(maleate)_3} \xrightarrow[\text{DTA(endo) 548 K}]{\text{TG 531–591 K}} \mathrm{Ni_2O_4(Imid)_4(maleate)}$

WL %th. 14.72 | WL %th. 27.65 | WL %th. 16.60

WL %exp. 14.8 | WL %exp. 27.7 | WL %exp. 16.6

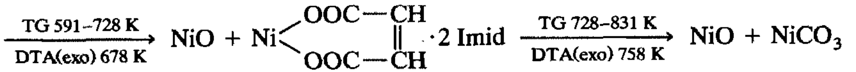

$\xrightarrow[\text{DTA(exo) 678 K}]{\text{TG 591–728 K}} \mathrm{NiO} + \mathrm{Ni}{<}\begin{array}{l}\mathrm{OOC{-}CH}\\ \qquad\quad \| \\ \mathrm{OOC{-}CH}\end{array} \cdot 2\ \mathrm{Imid} \xrightarrow[\text{DTA(exo) 758 K}]{\text{TG 728–831 K}} \mathrm{NiO} + \mathrm{NiCO_3}$

WL %th. 13.28 | WL %th. 13.71

WL %exp. 14.3 | WL %exp. 13.8

Total weight loss: theoretical 85.96%; experimental 87.2%.

Compound D

$\xrightarrow[\text{DTA(endo) 400 K}]{\text{TG 307–394 K}} \mathrm{Ni_2N_4(Imid)_5(maleate)_6NH_3} \xrightarrow[\text{DTA(endo) 453 K}]{\text{TG 394–460 K}} \mathrm{Ni_2(Imid)_5(maleate)_6} \xrightarrow[\text{DTA(endo) 553 K}]{\text{TG 460–557 K}} \mathrm{Ni_2(Imid)_4(maleate)_3} \xrightarrow[\text{DTA(endo) 618 K}]{\text{TG 557–604 K}}$

WL %th. 12.27 | WL %th. 5.25 | WL %th. 29.70

WL %exp. 12.3 | WL %exp. 4.8 | WL %exp. 29.9

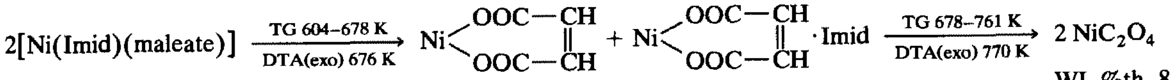

$\mathrm{2[Ni(Imid)(maleate)]} \xrightarrow[\text{DTA(exo) 676 K}]{\text{TG 604–678 K}} \mathrm{Ni}{<}\begin{array}{l}\mathrm{OOC{-}CH}\\ \qquad\quad \| \\ \mathrm{OOC{-}CH}\end{array} + \mathrm{Ni}{<}\begin{array}{l}\mathrm{OOC{-}CH}\\ \qquad\quad \| \\ \mathrm{OOC{-}CH}\end{array} \cdot \mathrm{Imid} \xrightarrow[\text{DTA(exo) 770 K}]{\text{TG 678–761 K}} 2\ \mathrm{NiC_2O_4}$

WL %th. 18.05 | WL %th. 4.89 | WL %th. 8.63

WL %exp. 17.1 | WL %exp. 4.8 | WL %exp. 10.4

$\xrightarrow[\text{DTA(exo)}]{\text{TG 761–831 K}} \mathrm{2NiCO_3}$

WL %th. 4.03

WL %exp. 3.1

Total weight loss: theoretical 82.93%; experimental 82.4%.

Exhibit 1 (continued)

Compound E

$\xrightarrow[\text{DTA(endo) 393 K}]{\text{TG 311–390 K}}$ $Ni_2N_4(Imid)_3(glutarate)_6 \cdot 5NH_3$ $\xrightarrow[\text{DTA(endo) 441 K}]{\text{TG 390–454 K}}$ $Ni_2N_4(Imid)_3(glutarate)_6 \cdot 3NH_3$ $\xrightarrow[\text{DTA(endo) 546 K}]{\text{TG 454–555 K}}$ $Ni_2N_2(Imid)_2(glutarate)_4$

WL %th. 12 | WL %th. 2.40 | WL %th. 28.84

WL %exp. 11.4 | WL %exp. 2.2 | WL %exp. 29.1

$\xrightarrow[\text{DTA(endo) 598 K}]{\text{TG 555–596 K}}$ $Ni(HOOC{-}(CH_2)_3{-}COO)_2 + Ni\begin{matrix} \diagup OOC{-}(CH_2)_3{-}COOH \\ \diagdown OOC{-}COOH \end{matrix}$ $\xrightarrow[\text{DTA(endo) 643 K}]{\text{TG 596–655 K}}$

WL %th. 14.52

WL %exp. 14.5

$Ni\begin{matrix} \diagup OOC{-}(CH_2)_3{-}COOH \\ \diagdown OOC{-}COOH \end{matrix} + Ni[HOOC{-}(CH_2){-}COO]_2$ $\xrightarrow[\text{DTA(exo) 678–683 K}]{\text{TG 655–670 K}}$ $Ni\begin{matrix} \diagup OOC{-}(CH_2)_3{-}COOH \\ \diagdown OOC{-}COOH \end{matrix} + NiCO_3$

WL %th. 3.95 | WL %th. 10.30

WL %exp. 4.0 | WL %exp. 10.1

$\xrightarrow[\text{DTA(exo) 743 K}]{\text{TG 670–756 K}}$ $NiO + NiCO_3$

WL %th. 14.38

WL %exp. 14.5

Total weight loss: theoretical 86.65%; experimental 85.8%.

Thermal studies

Additional studies were carried out by thermogravimetry to confirm the molecular formulae. The measurements were performed in air over the temperature range 293–1293 K at a heating rate of 10 K min^{-1} using a SETARAM T.G.85 microbalance. The differential thermal analyses were performed on a micro A.T.D. M4 using a heating rate of 4 K min^{-1}. Thermoanalytical diagrams for the complexes are shown in Figs. 1 and 2.

The general scheme of decomposition of the different complexes is summarized in the mechanisms shown in Exhibit 1 (WL = weight loss). Often the final stage of the decomposition forms the nickel carbonate or a mixture of nickel oxide with nickel carbonate.

Diffuse reflectance spectra

Diffuse reflectance spectra were recorded at room temperature for all compounds on a Beckman UV 5240 spectrophotometer over the range 40 000–4 000 cm^{-1}. Kodak white reflectance standard was used as a reference and for the dilution of nickel samples (10% by weight of nickel samples). In the near IR region, sharp peaks of weak intensity correspond to harmonics and combination bands of fundamental vibrations in the ligands. These bands are very difficult to assign. Two types of spectra have been recorded and are shown in Fig. 3. The electronic transitions observed and calculated for the different compounds are in Table 2.

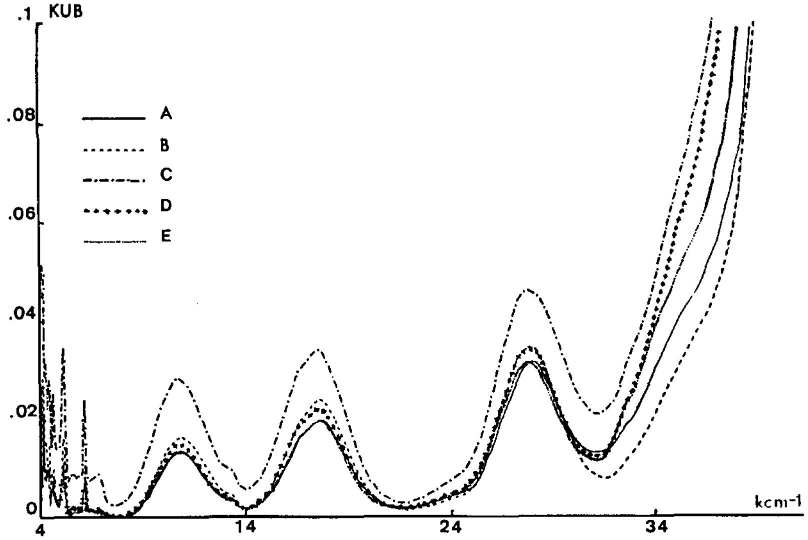

Fig. 3. Reflectance spectra.

TABLE 2

Electronic transitions (cm^{-1}) observed and calculated for the different complexes

Transition		Compound				
		A	B	C	D	E
ν_1	exp.	10691	10767	10806	10682	10737
$^3A_{2g}(F) \rightarrow {}^3T_{2g}(F)$	calc.	10614	10511	10702	10508	10603
Shoulder	exp.	13443	13473	13398	13234	13368
$^3A_{2g}(F) \rightarrow {}^1E_g$	calc.	13554	13340	13929	13628	13135
$\nu_3 - \nu_1$	exp.	16571	16631	16519	16357	16556
$^3T_{2g}(F) \rightarrow {}^1T_{2g}(P)$	calc.	17187	17156	17017	17273	16752
ν_2	exp.	17684	17586	17283	17523	17646
$^3A_{2g}(F) \rightarrow {}^3T_{1g}(F)$	calc.	17413	17161	17356	17240	17249
Shoulder	exp.	23849	23624	23774	24090	23789
$^3A_{2g}(F) \rightarrow {}^1T_{2g}(P)$	calc.	22535	22470	23273	22736	22074
ν_3^*	exp.	27914 *	27458	27582 *	27393	27232
$^3A_{2g}(F) \rightarrow {}^3T_{1g}(P)$	calc.	27801	27240	27719	27438	26942
ν_3^*	exp.		27834 *	28510	27724 *	27741 *
$^3A_{2g}(F) \rightarrow {}^1T_{1g}(G)$	calc.		27667	28488	27781	27305
$^3A_{2g}(F) \rightarrow {}^1T_{2g}$	exp.	35954	34751 35954	36030	35607	34600
$^3A_{2g}(F) \rightarrow {}^1E_g$	calc.	34747	34407 34821	36000	35077	33944
D_q		1136.2	1134.0	1096.3	1122.4	1141.0
B		767.5	760	798.4	771.7	743.8

The electronic spectra of all the complexes show a ν_3 band in the region near 27000 cm^{-1} due to the $^3A_{2g}(F) \rightarrow {}^3T_{1g}$ (P or G) transition, a ν_2 band around 17000 cm^{-1} due to the $^3A_{2g}(F) \rightarrow {}^3T_{1g}(F)$ transition and a ν_1 band around 10500 cm^{-1} due to the $^3A_{2g}(F) \rightarrow {}^3T_{2g}(F)$ transition. Though this assignment seems to be the most reasonable one, it does not account for the weak shoulder at around 13000 cm^{-1}, which appears to be due to a spin forbidden transition. It is possible that the ligand field in this complex is distorted from true octahedral symmetry and that the low symmetry component splits the $^3A_{2g}(F) \rightarrow {}^3T_{2g}(F)$ transition giving the spin allowed band $^3A_{2g}(F) \rightarrow {}^1E_g(1D)$. For octahedral nickel(II) complexes where the ν_2 and ν_3 bands were observed the Racah parameters B can be deduced. D_q and B were found by using the following equations [11]

$$340\, D_q^2 - 18(\nu_2 + \nu_3)D_q + \nu_2\nu_3 = 0$$

and

$$B = \frac{\nu_3 + \nu_2 - 30\, D_q}{15}$$

Δ_0 is, of course, always the energy of the first transition for a d^8 ion; the value of Δ_0/B [12] leads to the position of the different transitions. The values of the predicted transitions appear to be in good agreement with the observed values (Table 2).

It seems that the octahedral environment is not affected by the carboxylic acid or by oxygen or nitrogen molecules.

REFERENCES

1 R.G. Wilkins, Uptake of oxygen by cobalt(II) complexes in solutions, Adv. Chem. Ser., 100 (1971) 111.

2 J.S. Valentine, The dioxygen ligand in mononuclear group VIII transition metal complexes, Chem. Rev., 73 (1973) 235.

3 Yu.I. Bratushko and K.B. Yatsimirskii, Coordination compounds of 3d transition metals with molecular oxygen (collected papers), Usp. Khim. Koord. Soedin., (1975) 7.

4 A.V. Savitskii and V.I. Nelyubin, The activation of molecular oxygen with transition metal complexes, Usp. Khim., 44 (1975) 214; Russ. Chem. Rev. (Engl. Transl.), 44 (1975) 2.

5 J.P. Collman, Synthetic models for the oxygen-binding hemoproteins, Chem. Rev., 10 (1977) 265.

6 G. McLendon and A.E. Martell, Inorganic oxygen carriers as models for biological systems, Coord. Chem. Rev., 19 (1976) 1.

7 L. Vaska, Dioxygen metal complexes, Acc. Chem. Res., 9 (1976) 175.

8 Yu.I. Bratushko and N.G. Mel'nikova, Preparation and properties of aminoacid-imidazole complexes of cobalt with molecular oxygen, Russ. J. Inorg. Chem. (Engl. Transl.), 26(11) (1981) 1607.

9 D. Burk, J.Z. Hearon, L. Caroline and A.L. Schade, J. Biol. Chem., 165 (1946) 723; E.C. Niederhoffer, J.T. Timmons and A.E. Martell, Chem. Rev., 84 (1984) 137.

10 S. Sakaki, K. Morokuma and K. Ohkubo, Ab initio MO study of the coordination modes and bonding nature of $Rh^I–N_2$ complexes, J. Am. Chem. Soc., 107 (1985) 2686.

11 A.E. Underhill and D.E. Billing, Calculations of the Racah parameter B for nickel(II) and cobalt(II) compounds, Nature (London), 5038 (1966) 835.

12 Y. Tanabe and S. Sugano, J. Phys. Soc. Jpn., 9 (1954) 753; 9 (1954) 766.